

# Using intestinal flora to distinguish non-alcoholic steatohepatitis from non-alcoholic fatty liver

Chao Li<sup>1,2</sup>, Lihong Cui<sup>1,2</sup> , Xiaohui Wang<sup>2</sup>,  
Zihui Yan<sup>2</sup>, Shaoxin Wang<sup>2</sup> and Yan Zheng<sup>2</sup>

## Abstract

**Objective:** To explore specific flora in mouse models of non-alcoholic steatohepatitis (NASH) to improve NASH diagnostic protocols.

**Methods:** Sixty mice were divided into normal diet (ND, 20 mice) and high-fat/high-sugar diet (HFSD) groups (40 mice). After 8 weeks of feeding, 10 mice in the ND group and 20 mice in the HFSD group were sacrificed to create the short-term ND and non-alcoholic fatty liver (NAFL) groups, respectively. After 16 weeks of feeding, the remaining mice were sacrificed to create the long-term ND and NASH groups, respectively. We then examined fecal flora, serum biochemical indices, and lipopolysaccharide and tumor necrosis factor- $\alpha$  levels and analyzed liver tissue.

**Results:** The relative abundance of *Lactobacillus*, *Desulfovibrio*, *Ruminiclostridium 9*, and *Turicibacter* differed between NASH and NAFL mice, and the areas under the receiver operating characteristic curve of the four genera for diagnosing NASH were 0.705, 0.734, 0.737, and 0.937. The non-alcoholic fatty liver disease activity score was positively correlated with the relative abundance of *Desulfovibrio* ( $r = 0.353$ ), *Ruminiclostridium 9* ( $r = 0.431$ ), and *Turicibacter* ( $r = 0.688$ ).

**Conclusions:** The relative abundance of *Lactobacillus*, *Desulfovibrio*, *Ruminiclostridium*, and *Turicibacter* may help distinguish NASH from NAFL.

## Keywords

Non-alcoholic fatty liver disease, non-alcoholic steatohepatitis, intestinal flora, high fat/high sugar diet, endotoxin, *Lactobacillus*, *Desulfovibrio*, *Ruminiclostridium*, *Turicibacter*

Date received: 29 July 2020; accepted: 9 November 2020

## Corresponding author:

Lihong Cui, Medical School of Chinese PLA, Beijing 100853, China; Department of Gastroenterology, the Sixth Medical Center, Chinese PLA General Hospital, No. 6 Fucheng Road, Haidian District, Beijing 100048, China.  
Email: cuilhkeyan@163.com

<sup>1</sup>Medical School of Chinese PLA, Beijing, China

<sup>2</sup>Department of Gastroenterology, the Sixth Medical Center, Chinese PLA General Hospital, Beijing, China



## Introduction

Non-alcoholic fatty liver disease (NAFLD) affects more than 30% of people in Western societies, and its prevalence in obese patients is as high as 75%.<sup>1-3</sup> Non-alcoholic fatty liver (NAFL) and non-alcoholic steatohepatitis (NASH) are different forms of NAFLD, and they can be distinguished *via* histological examination of the liver.<sup>4</sup> In total, 10% to 20% of patients with NAFL will progress to NASH, and one-third of patients with NASH will progress to liver cirrhosis, a major risk factor for the development of hepatocellular carcinoma, within 5 to 10 years.<sup>5,6</sup> Thus, early diagnosis of NASH is critical to allow interventions that may limit progression. However, many limitations exist in current NASH diagnostic protocols. The diagnosis of NASH usually relies on histologic liver examination, requiring liver biopsy, which is not well accepted by patients because of its invasive nature and corresponding risk. Less invasive methods of NASH diagnosis have not been developed or verified compared with biopsy diagnoses.

The intestinal flora comprises the gastrointestinal symbionts of the host, and it plays critical roles in host energy metabolism.<sup>7</sup> Studies on the relationship between the intestinal flora and NAFLD provides a framework that could be used to diagnose NASH using less invasive methods. Clinical studies revealed that the proportion of small intestine bacterial overgrowth in patients NAFLD is significantly higher than that of healthy people.<sup>8</sup> Additionally, regulation of the intestinal flora using probiotics, prebiotics, and antibiotics can lead to improvements of both NAFL and NASH<sup>9-11</sup> in patients. However, few studies have explored the intestinal flora at the genus level to understand the role of these bacteria in the pathogenesis of NAFLD or to distinguish NASH from NAFL.

In our study, we investigated which bacteria are closely associated with NAFL and

NASH in the intestinal flora of mice at the genus level. We then examined which specific bacteria have potential diagnostic value for differentiating NASH from NAFL.

## Materials and methods

### Experimental animal models

Sixty male specific-pathogen-free C57BL/6J mice (8 weeks old; weight,  $20 \pm 2$  g) were purchased from Weishang Lituo Technology Co., LTD (Beijing, China). The mice were housed in a controlled environment at a temperature of  $22 \pm 2^\circ\text{C}$ , relative humidity of 50% to 60%, and a 12-hour/12-hour light/dark cycle. We used independent ventilation cages, and mice were housed five per cage. All experiments were conducted in accordance with the National Institutes of Health guidelines for the care and use of laboratory animals.

### Experiment group protocols

After 2 weeks of adaptation to the new environment, mice were randomly divided into two groups using a random number table. Twenty mice were assigned to the normal diet (ND) group, which received a standard chow diet (fat provided 10% of total energy) and pure water. The standard chow diet was purchased from Jiangsu Synergetic Pharmaceutical Bio-engineering Co., LTD (Jiangsu, China). Forty mice were assigned to the high-fat/high-sugar diet (HFSD) group, which received high-fat chow (fat provided 42% energy) and “sugary” drinks (each liter of water contained 18.9 g of sucrose and 23.1 g of fructose). The high-fat chow (formula TP26300) was purchased from Nantong Teluofei Feed Technology Co., LTD (Jiangsu, China). Both groups of mice had *ad libitum* access to food and water. After 8 weeks of feeding, 10 mice in the ND group and 20

mice in the HSDS group were sacrificed to create the short-term ND (STND) and NAFL groups, respectively. After 16 weeks of feeding, the remaining mice were sacrificed to create the long-term ND (LTND) and NASH groups, respectively. Fresh blood and fecal samples were collected prior to mouse sacrifice, at which point liver tissue was collected.

### Sample collection

Metabolic cages were used to collect fresh feces. The mice were overnight fasted before blood samples were collected *via* posterior orbital venous plexus puncture. After collecting blood samples, mice were sacrificed using carbon dioxide. Mouse livers were then removed and fixed for 24 hours in 4% paraformaldehyde for further histological examination.

### Histological examination of the liver

Pathological sections of mouse liver were examined by an experienced pathologist who was blinded to the research, and

slides were stained with hematoxylin–eosin (HE) and picrosirius red. Microscopic images were acquired using a Nikon Eclipse E100 microscope system (Nikon, Tokyo, Japan). NAFLD was diagnosed by the presence of fatty hepatocytes occupying more than 5% of the hepatic parenchyma.<sup>12</sup> NAFLD was further classified as NAFL or NASH according to the Matteoni classification system<sup>13</sup> and the NAFLD activity score (NAS).<sup>14</sup> The Matteoni classification method includes the following disease states: type 1, simple steatosis; type 2, steatosis and lobular inflammation; type 3, steatosis and ballooning degeneration of hepatocyte; and type 4, type 3 plus either Mallory hyaline or fibrosis. Matteoni types 1 and 2 were diagnosed as NAFL, and types 3 and 4 were diagnosed as NASH. The NAS scoring criteria are presented in Table 1.

### Blood analysis

Serum total cholesterol (TC), triglyceride (TG), high-density lipoprotein cholesterol (HDL-C), low-density lipoprotein

**Table 1.** NAFLD Activity Score.

Histologic appearance	Features	Score
Hepatocyte ballooning	None	0
	Few ballooning cells	1
	Many cells/prominent ballooning	2
Lobular inflammation	No foci	0
	<2 foci per ×200 field	1
	2–4 foci per ×200 field	2
	>4 foci per ×200 field	3
Steatosis	<5%	0
	5%–33%	1
	33%–66%	2
	>66%	3
Pathologic diagnosis		Total score
Probable or definite NASH		≥5
Uncertain		3–4
Not NASH		≤2

NAFLD, non-alcoholic fatty liver disease activity score; NASH, non-alcoholic steatohepatitis.

cholesterol (LDL-C), alanine aminotransferase (ALT), aspartate aminotransferase (AST), and fasting blood glucose (FBG) levels in mice were detected using a commercial kit (Nanjing Jiancheng Institute of Biological Engineering, Nanjing, China). Serum tumor necrosis factor- $\alpha$  (TNF- $\alpha$ ) and lipopolysaccharide (LPS) levels were detected using an ELISA kit (Abbkine, Wuhan, China). Both analyses were conducted according to the manufacturers' instructions.

### ***Fecal DNA extraction and high-throughput sequencing***

DNA extraction from feces was performed using a QIAamp Fast DNA Stool Mini Kit (QIAGEN, Hilden, Germany) according to the manufacturer's instructions. The V3-4 hypervariable region of the bacterial 16S rRNA gene was amplified using the primers 338F (ACTCCTACGGGAGGCAGCAG) and 806R (GGACTACHVGGGTW TCTAAT).<sup>15</sup> PCR products were purified using an Agencourt AMPure XP Kit (Beckman Coulter, Brea, CA, USA). Deep sequencing was performed on a MiSeq platform at Allwegene Company (Beijing, China). Image analysis and error estimation were performed using Illumina Analysis Pipeline Version 2.6 (Illumina, Brea, CA, USA).

### ***Data analyses***

Qiime and vsearch software were used to conduct bioinformatics statistical analysis. Sequences were clustered into operational taxonomic units (OTUs) at a similarity level of 97%.<sup>16</sup> Based on the OUT results, mothur was used to generate rarefaction curves and calculate richness and diversity indices. The Ribosomal Database Project classifier tool was used to classify all sequences into taxonomic groups (i.e., phylum, class, order, family, genus, species).<sup>17</sup>

Data are presented as the mean  $\pm$  SD, and SPSS software version 19.0 (IBM, Armonk, NY, USA) was used to analyze the data. A two-tailed Student's *t*-test was used for statistical analysis to compare differences between two groups of normally distributed data. ANOVA was performed to compare data from multiple groups that were normally distributed and that had homogenous variance. For non-normally distributed or homogenous data, the Kruskal–Wallis test and Tamhane's T2 test were used to compare multiple groups of data. Receiver operating characteristic (ROC) curve analysis was conducted using SPSS. Correlation analysis was performed using Spearman's correlation.  $P < 0.05$  was considered statistically significant.

## **Results**

### ***Establishment of NAFL/NASH mouse models using a high fat/high sugar diet***

After 8 and 16 weeks of feeding, HE staining of pathological sections from the ND group revealed a clear hepatic lobule structure with an orderly arrangement of liver plates and no steatosis or hepatocyte damage. Picrosirius red staining disclosed no obvious collagenous fiber hyperplasia (STND-1, STND-2, LTND-1, and LTND-2, Figure 1). After 8 weeks, HE staining of pathological sections from the HFSD group revealed hepatocyte steatosis, vacuoles of different sizes in the cytoplasm, hepatocyte edema, and lightly stained and loose cytoplasm. However, picrosirius red staining revealed no obvious collagenous fiber hyperplasia, as observed in the ND group (NAFL-1 and NAFL-2, Figure 1). After 16 weeks, HE staining of pathological sections from the HFSD group uncovered extensive hepatocyte steatosis, scattered neutrophils infiltrating small foci, and ballooning degeneration of some hepatocytes. In this group, picrosirius red staining revealed

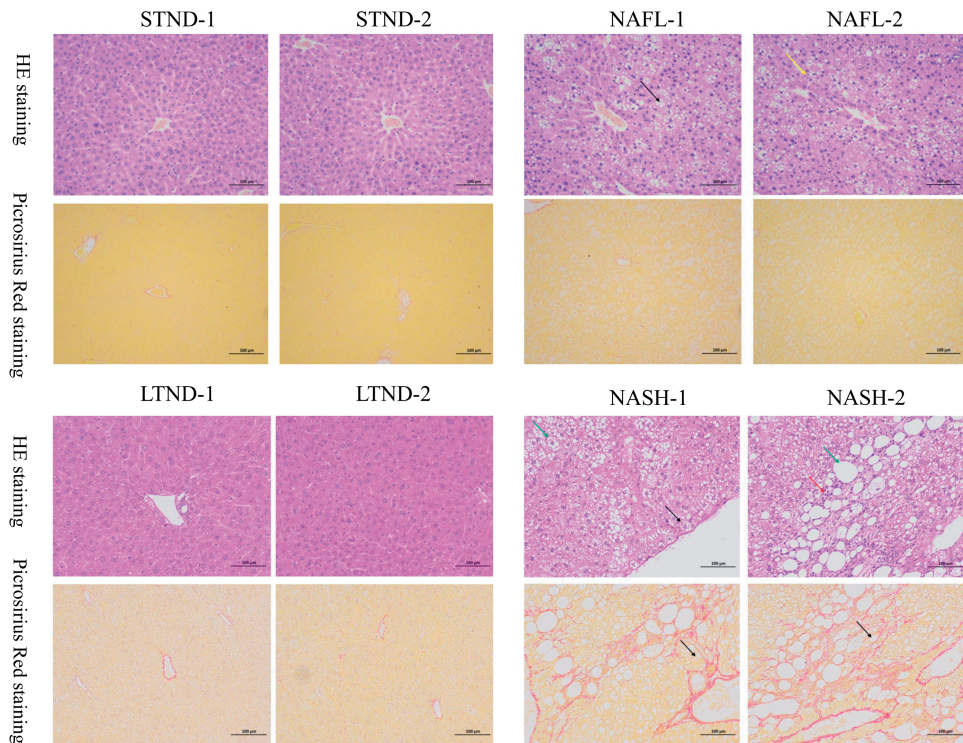


**Figure 1.** Microscopic assessment of liver histology. Mice from the STND, LTND, NAFL, and NASH groups are presented. Two representative photographs of mice stained with HE and picrosirius red are presented. In the NAFL group, black arrows point to vacuoles in the cytoplasm, and yellow arrows identify lightly stained and loose cytoplasm. In the NASH group, green arrows denote vacuoles in the cytoplasm, and the red arrow identifies scattered neutrophil infiltrate. The black arrow in the HE-stained image reveals ballooning degeneration of a hepatocyte, and the black arrow in the picrosirius red-stained image identifies local collagenous fiber hyperplasia around the portal tracts and hepatic sinusoids. STND, short-term normal diet; LTND, long-term normal diet; NAFL, non-alcoholic fatty liver; NASH, non-alcoholic steatohepatitis; HE, hematoxylin-eosin.

local collagenous fiber hyperplasia around the portal tracts and hepatic sinusoids (NASH-1 and NASH-2, Figure 1). After 8 weeks, the pathological features of the livers of 13 mice in the HFSD group conformed to type 1 of the Matteoni classification, and the remaining seven mice were classified into type 2. After 16 weeks, the pathological features of the livers of 15 mice in the HFSD group conformed to type 3 of the Matteoni classification, and the remaining five mice conformed to type 4. According to the Matteoni classification, the HFSD group developed NAFL within

8 weeks and progressed to NASH after another 8 weeks. Furthermore, we compared the NAS between the NAFL and NASH groups. NAS in the NAFL group was  $1.90 \pm 0.85$ , versus  $5.33 \pm 1.08$  in the NASH group ( $P < 0.01$ ).

#### *Variation in serum biochemical indexes and LPS and TNF- $\alpha$ levels in mouse models of NAFL/NASH*

Serum TG, LDL-C, and AST levels were higher in the NAFL and NASH groups than in the STND and LTND group

**Table 2.** Variations of serum biochemical indices, LPS, and TNF- $\alpha$ .

Serum indexes	STND	LTND	NAFL	NASH
TC (mmol/L)	3.84 $\pm$ 0.73 <sup>cd</sup>	3.96 $\pm$ 0.53 <sup>d</sup>	4.95 $\pm$ 1.37 <sup>a</sup>	5.74 $\pm$ 1.39 <sup>ab</sup>
TG (mmol/L)	0.65 $\pm$ 0.12 <sup>cd</sup>	0.70 $\pm$ 0.13 <sup>cd</sup>	0.97 $\pm$ 0.31 <sup>ab</sup>	1.10 $\pm$ 0.49 <sup>ab</sup>
HDL-C (mmol/L)	1.39 $\pm$ 0.75	1.26 $\pm$ 0.52	1.22 $\pm$ 0.55	1.10 $\pm$ 0.74
LDL-C (mmol/L)	0.35 $\pm$ 0.18 <sup>cd</sup>	0.36 $\pm$ 0.10 <sup>cd</sup>	0.63 $\pm$ 0.15 <sup>ab</sup>	0.75 $\pm$ 0.25 <sup>ab</sup>
ALT (KarU)	37.55 $\pm$ 8.47 <sup>cd</sup>	42.32 $\pm$ 21.21 <sup>d</sup>	68.11 $\pm$ 24.81 <sup>a</sup>	80.49 $\pm$ 17.33 <sup>ab</sup>
AST (KarU)	34.26 $\pm$ 9.68 <sup>cd</sup>	37.88 $\pm$ 17.54 <sup>cd</sup>	55.96 $\pm$ 18.55 <sup>ab</sup>	65.64 $\pm$ 18.40 <sup>ab</sup>
FBG (mmol/L)	6.41 $\pm$ 1.28 <sup>d</sup>	6.58 $\pm$ 0.89 <sup>d</sup>	7.95 $\pm$ 2.38	9.00 $\pm$ 2.04 <sup>ab</sup>
LPS (ng/L)	237.49 $\pm$ 10.13 <sup>cd</sup>	239.71 $\pm$ 15.78 <sup>d</sup>	256.16 $\pm$ 24.41 <sup>ad</sup>	282.80 $\pm$ 29.47 <sup>abc</sup>
TNF- $\alpha$ (pg/mL)	18.96 $\pm$ 1.64	18.85 $\pm$ 2.64	20.36 $\pm$ 4.33	19.97 $\pm$ 2.96

Note: <sup>a</sup> $P < 0.05$ , versus STND group; <sup>b</sup> $P < 0.05$ , versus LTND group; <sup>c</sup> $P < 0.05$ , versus NAFL group; <sup>d</sup> $P < 0.05$ , versus NASH group.

TC, total cholesterol; TG, triglyceride; HDL-C, high-density lipoprotein cholesterol; LDL-C, low-density lipoprotein cholesterol; ALT, alanine aminotransferase; AST, aspartate aminotransferase; FBG, fasting blood glucose; LPS, lipopolysaccharide; TNF- $\alpha$ , tumor necrosis factor- $\alpha$ ; STND, short-term normal diet; LTND, long-term normal diet; NAFL, non-alcoholic fatty liver; NASH, non-alcoholic steatohepatitis.

(all  $P < 0.05$ ). Serum ALT and TC levels were also significantly higher in the NAFL group than in the STND group and significantly higher in the NASH group than in the LTND group (all  $P < 0.05$ ). Additionally, serum FBG levels were significantly higher in the NASH group than in the STND and LTND groups (both  $P < 0.05$ ). These data are summarized in Table 2 and Figure 2a–g.

We also found that serum LPS levels were significantly higher in the NAFL group than in the STND group and significantly higher in the NASH group than in the LTND group (both  $P < 0.05$ ). Within the NAFLD group, serum LPS levels were higher in the NASH group than in the NAFL group ( $P < 0.05$ ). However, TNF- $\alpha$  levels were indistinguishable between the groups (Table 2, Figure 2h–i).

### Abundance and diversity of fecal flora in NAFLD mouse models

In total, 2,946,996 high-quality sequences were obtained from the fecal samples with a mean of  $50,810 \pm 30,473$  sequences per sample (range, 20,129–192,272). These sequences clustered into 1500 OTUs, of

which 1459 OTUs were assigned using the Greengenes database. Only 383 OTUs (26.25%) were shared by the four groups (Figure 3a). The NAFL and NASH groups accounted for 164 and 44 unique OTUs, respectively.

The Chao1 and Shannon indices are important statistical analysis indices of  $\alpha$  diversity, which can reflect the abundance and diversity of microbial communities. The Chao1 and Shannon indices of the NAFL and NASH groups were significantly lower than those of the STND and LTND groups (all  $P < 0.05$ ). However, there was no significant difference in either index between the NASH and NAFL groups (Figure 3b).

Principal component analysis (PCA) and principal coordinates analysis (PCoA) are commonly used methods for  $\beta$  diversity analysis, which compares the microbial community composition of samples from different groups. PCA and PCoA demonstrated that the fecal flora structure of the NAFL and NASH groups were more similar than those of the STND and LTND groups. However, there was no obvious difference in the fecal flora structure between the NAFL and NASH groups (Figure 3c).

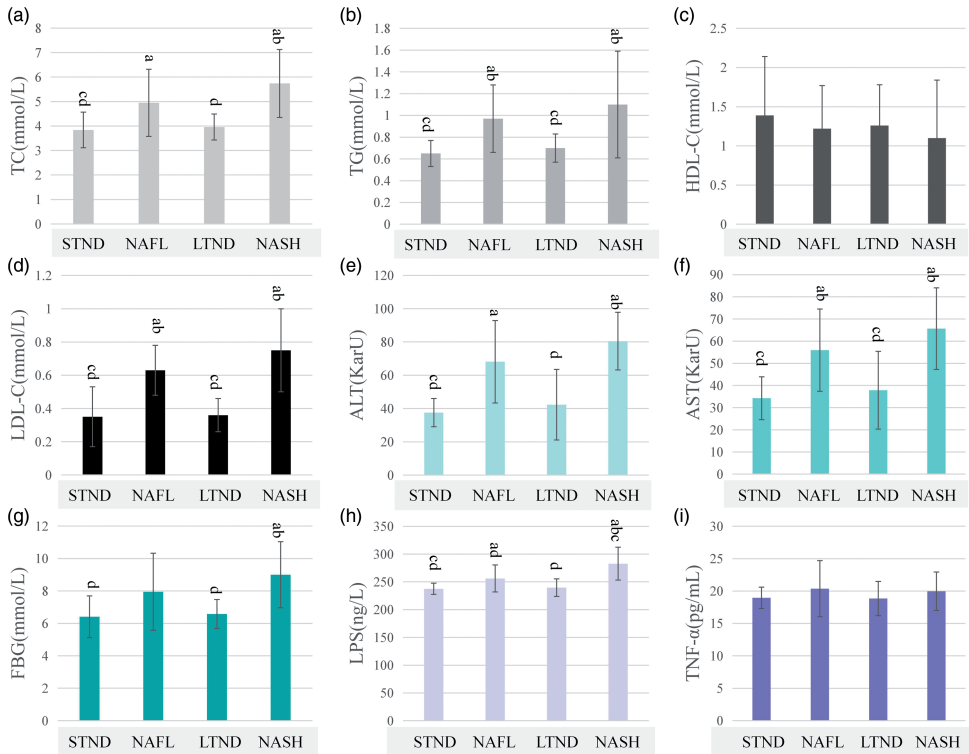


**Figure 2.** a) Serum TC, b) TG, c) HDL-C, d) LDL-C, e) ALT, f) AST, g) FBG, h) LPS, and i) TNF- $\alpha$  levels of mice in the STND, LTND, NAFL, and NASH groups. Data represent the mean  $\pm$  SD of each group. <sup>a</sup>P < 0.05, versus STND group; <sup>b</sup>P < 0.05, versus LTND group; <sup>c</sup>P < 0.05, versus NAFL group; <sup>d</sup>P < 0.05, versus NASH group.

TC, total cholesterol; TG, triglyceride; HDL-C, high-density lipoprotein cholesterol; LDL-C, low-density lipoprotein cholesterol; ALT, alanine aminotransferase; AST, aspartate aminotransferase; FBG, fasting blood glucose; LPS, lipopolysaccharide; TNF- $\alpha$ , tumor necrosis factor- $\alpha$ ; STND, short-term normal diet; LTND, long-term normal diet; NAFL, non-alcoholic fatty liver; NASH, non-alcoholic steatohepatitis.

### Taxonomic analysis of fecal flora composition in NAFLD mouse models

We identified 19 bacterial phyla in our analysis. We focused additional analyses on bacterial phyla with a relative abundance exceeding 1%, which included Bacteroidetes, Firmicutes, Proteobacteria, Actinobacteria, and Saccharibacteria. We found that the relative abundance of Firmicutes and Actinobacteria was significantly higher in the NAFL and NASH groups than in the STND and LTND groups (all  $P < 0.05$ ), whereas that of

Bacteroidetes and Saccharibacteria was significantly lower (all  $P < 0.05$ ). The relative abundance of Proteobacteria in the NASH group was also significantly higher ( $P < 0.05$ ) than that in the STND and LTND groups. We did not identify any differences in the relative abundance of these five phyla when between the NAFL and NASH groups (Table 3, Figure 4a).

We detected 221 bacterial genera, and similarly as our phyla analyses, we focused on genera with a relative abundance exceeding 1%. The relative abundance of *Alloprevotella*, *Ruminococcaceae* UCG-014,

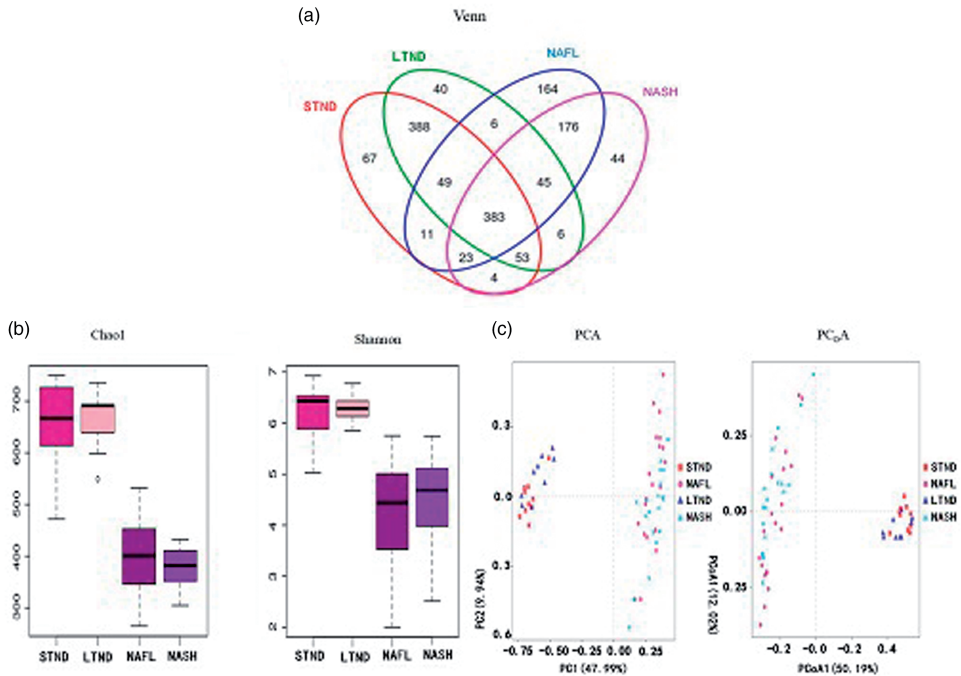


**Figure 3.** a) Venn diagram of fecal flora OTUs of the STND, LTND, NAFL, and NASH groups. b) Chao I and Shannon indices of the fecal flora of each group. c) OTUs-based PCA and Bray–Curtis-based PCoA of the fecal flora of the four groups.

OTU, operational taxonomic unit; STND, short-term normal diet; LTND, long-term normal diet; NAFL, non-alcoholic fatty liver; NASH, non-alcoholic steatohepatitis; PCA, principal component analysis, PCoA, principal coordinates analysis.

**Table 3.** Variations in the relative abundance of phyla.

Phylum	STND	LTND	NAFL	NASH
Firmicutes	30.60 ± 10.51 <sup>cd</sup>	34.42 ± 6.89 <sup>cd</sup>	64.40 ± 8.38 <sup>ab</sup>	65.63 ± 9.63 <sup>ab</sup>
Bacteroidetes	62.22 ± 11.42 <sup>cd</sup>	56.58 ± 6.22 <sup>cd</sup>	8.94 ± 8.13 <sup>ab</sup>	7.21 ± 6.07 <sup>ab</sup>
Actinobacteria	1.92 ± 1.33 <sup>bcd</sup>	5.08 ± 2.50 <sup>acd</sup>	17.82 ± 8.92 <sup>ab</sup>	17.94 ± 7.19 <sup>ab</sup>
Proteobacteria	2.71 ± 1.39 <sup>d</sup>	2.21 ± 0.77 <sup>d</sup>	7.22 ± 7.74	7.60 ± 4.07 <sup>ab</sup>
Saccharibacteria	1.41 ± 0.82 <sup>cd</sup>	1.14 ± 0.42 <sup>cd</sup>	0.02 ± 0.02 <sup>ab</sup>	0.03 ± 0.04 <sup>ab</sup>

Note: <sup>a</sup> $P < 0.05$ , versus STND group; <sup>b</sup> $P < 0.05$ , versus LTND group; <sup>c</sup> $P < 0.05$ , versus NAFL group; <sup>d</sup> $P < 0.05$ , versus NASH group.

STND, short-term normal diet; LTND, long-term normal diet; NAFL, non-alcoholic fatty liver; NASH, non-alcoholic steatohepatitis.

*Ruminococcus* 1, and *Candidatus Saccharimonas* were significantly higher in the STND and LTND groups than in the NAFL and NASH groups (all  $P < 0.05$ ).

Conversely, the relative abundance of *Bifidobacterium*, *Faecalibaculum*, *Helicobacter*, *Eubacterium coprostanoligenes* group, and *Romboutsia* was

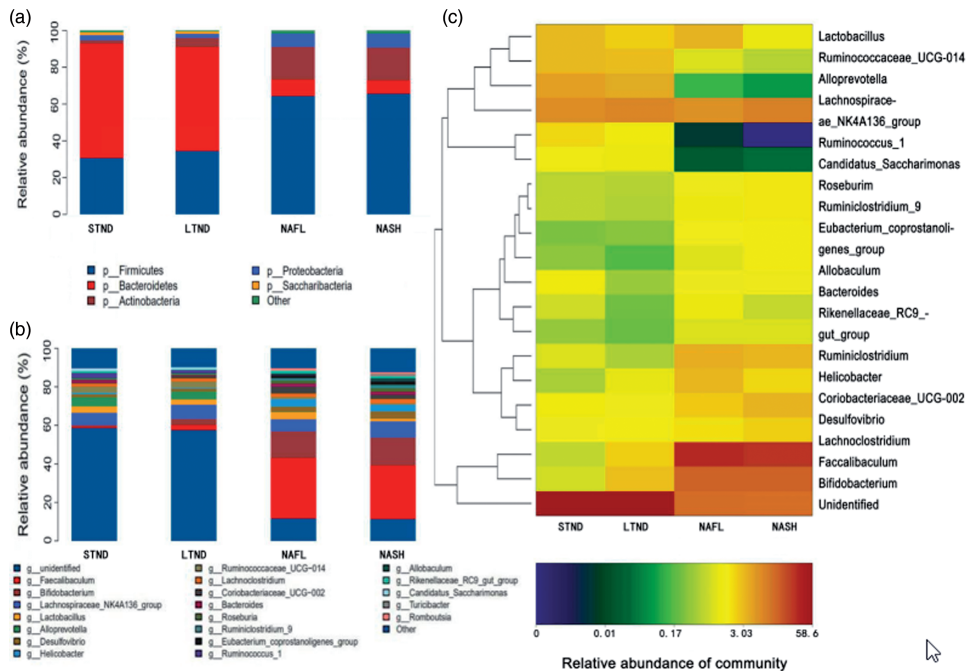


**Figure 4.** Relative abundance of fecal flora in the STND, LTND, NAFL, and NASH groups at the a) phylum and b) genus levels. c) Heatmap of the top 20 genera in the fecal flora of mice reflecting clustering similarities. Genera with high and low abundance can be clustered in blocks that reflect the similarities or differences across samples and classification levels. STND, short-term normal diet; LTND, long-term normal diet; NAFL, non-alcoholic fatty liver; NASH, non-alcoholic steatohepatitis.

significantly lower in the STND and LTND groups than in the NAFL and NASH groups (all  $P < 0.05$ ; Table 4, Figure 4b and c).

We also identified a difference in the relative abundance of four genera that could be used to distinguish the NAFL and NASH groups. Compared with the NAFL group, the relative abundance of *Lactobacillus* in the NASH group was significantly lower ( $P < 0.05$ ), whereas that of *Desulfovibrio*, *Ruminiclostridium* 9, and *Turicibacter* was significantly higher (all  $P < 0.05$ ; Table 4). Using the relative abundance of these four genera, we plotted an ROC curve and calculated the area under the ROC curve (AUROC) to determine if these genera could be used to diagnose

NASH. The AUROCs of the four genera were 0.705, 0.734, 0.737, and 0.937, respectively (Figure 5). We also used Spearman's correlation to evaluate the NAS of the mice in the NAFL and NASH groups and the relative abundance of these four genera. This analysis revealed that NAS was positively correlated with the relative abundance of *Desulfovibrio* ( $r = 0.353$ ,  $P < 0.05$ ), *Ruminiclostridium* 9 ( $r = 0.431$ ,  $P < 0.01$ ), and *Turicibacter* ( $r = 0.688$ ,  $P < 0.01$ ) but not that of *Lactobacillus*.

## Discussion

The prevalence of NAFLD is increasing worldwide, and it is estimated that NAFLD will be the leading cause of

**Table 4.** Variations in the relative abundance of genera.

Genus	STND	LTND	NAFL	NASH
<i>Alloprevotella</i>	4.89 ± 2.37 <sup>cd</sup>	4.28 ± 1.89 <sup>cd</sup>	0.13 ± 0.26 <sup>ab</sup>	0.08 ± 0.11 <sup>ab</sup>
<i>Ruminococcaceae</i> UCG-014	3.22 ± 1.79 <sup>cd</sup>	3.20 ± 1.14 <sup>cd</sup>	0.94 ± 1.64 <sup>ab</sup>	0.55 ± 0.83 <sup>ab</sup>
<i>Ruminococcus</i> 1	2.17 ± 1.91 <sup>cd</sup>	1.32 ± 0.79 <sup>cd</sup>	<0.01 <sup>ab</sup>	<0.01 <sup>ab</sup>
<i>Candidatus Saccharimonas</i>	1.41 ± 0.82 <sup>cd</sup>	1.14 ± 0.42 <sup>cd</sup>	0.02 ± 0.02 <sup>ab</sup>	0.03 ± 0.04 <sup>ab</sup>
<i>Bifidobacterium</i>	0.83 ± 0.68 <sup>bcd</sup>	3.21 ± 1.57 <sup>acd</sup>	13.76 ± 7.96 <sup>ab</sup>	14.46 ± 6.01 <sup>ab</sup>
<i>Faecalibaculum</i>	0.65 ± 1.18 <sup>cd</sup>	2.53 ± 2.59 <sup>cd</sup>	31.60 ± 15.17 <sup>ab</sup>	27.85 ± 16.15 <sup>ab</sup>
<i>Helicobacter</i>	0.94 ± 0.60 <sup>cd</sup>	0.48 ± 0.44 <sup>cd</sup>	3.99 ± 3.56 <sup>ab</sup>	3.57 ± 3.20 <sup>ab</sup>
<i>Eubacterium coprostanoligenes</i> group	0.26 ± 0.22 <sup>cd</sup>	0.29 ± 0.26 <sup>cd</sup>	1.65 ± 1.70 <sup>ab</sup>	1.80 ± 1.74 <sup>ab</sup>
<i>Romboutsia</i>	<0.01 <sup>cd</sup>	<0.01 <sup>cd</sup>	1.01 ± 0.69 <sup>ab</sup>	0.75 ± 0.61 <sup>ab</sup>
<i>Lactobacillus</i>	3.22 ± 1.51 <sup>d</sup>	2.52 ± 1.11 <sup>d</sup>	3.68 ± 3.52 <sup>d</sup>	1.19 ± 0.89 <sup>abc</sup>
<i>Desulfovibrio</i>	1.31 ± 0.89 <sup>cd</sup>	1.44 ± 0.53 <sup>cd</sup>	2.68 ± 1.16 <sup>abd</sup>	3.75 ± 1.20 <sup>abc</sup>
<i>Ruminiclostridium</i> 9	0.61 ± 0.45 <sup>cd</sup>	0.51 ± 0.17 <sup>cd</sup>	1.26 ± 0.55 <sup>abd</sup>	1.84 ± 0.67 <sup>abc</sup>
<i>Turicibacter</i>	0.05 ± 0.11 <sup>d</sup>	0.06 ± 0.09 <sup>d</sup>	0.35 ± 1.23 <sup>d</sup>	1.45 ± 1.03 <sup>abc</sup>

Note: <sup>a</sup>P < 0.05, versus STND group; <sup>b</sup>P < 0.05, versus LTND group; <sup>c</sup>P < 0.05, versus NAFL group; <sup>d</sup>P < 0.05, versus NASH group.

STND, short-term normal diet; LTND, long-term normal diet; NAFL, non-alcoholic fatty liver; NASH, non-alcoholic steatohepatitis.

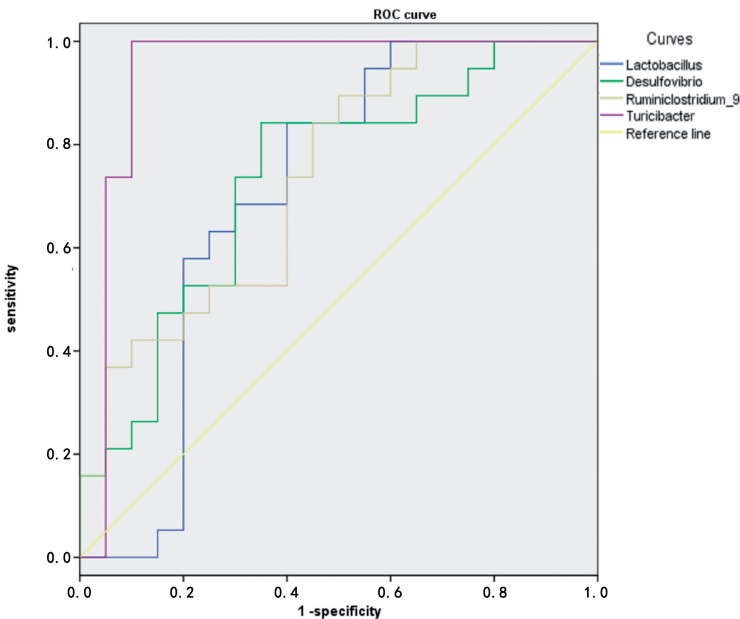


**Figure 5.** Receiver operating characteristic analysis of the relative abundance of *Lactobacillus*, *Desulfovibrio*, *Ruminiclostridium* 9, and *Turicibacter* for diagnosing non-alcoholic steatohepatitis.

cirrhosis and hepatocellular carcinoma within the next 5 years. Mouse models provide an opportunity to understand the pathogenetic mechanisms of NAFLD. We fed

mice a high-fat/high-sugar diet to establish a mouse model of NAFL/NASH. After 8 weeks of high-fat/high-sugar diet feeding, mice developed a liver pathology that

mimicked aspects of human NAFL/NASH, including hepatocyte steatosis and edema. After 16 weeks of high-fat/high-sugar diet feeding, mice exhibited a pathology consistent with NASH, including scattered neutrophils infiltrating small foci and ballooning degeneration of hepatocytes. The findings suggest that a high-fat/high-sugar diet can induce NAFL/NASH in mice.

In addition to the development of liver pathology consistent with NAFL/NASH, we found that a high-fat/high-sugar diet led to increased serum TG, TC, and LDL-C levels. Prior studies revealed that long-term consumption of a high-fat diet can lead to increased synthesis of TG, TC, and LDL-C that exceeds the rate of transport and metabolism in hepatocytes and that can lead to NAFLD and hyperlipemia.<sup>18,19</sup> In our model, the development of NASH (but not NAFL) was accompanied by an increase in FBG content.

ALT and AST are important indicators of liver function, and they are used as surrogate markers of liver damage. In the clinic, ALT and AST have also been used to non-invasively distinguish NAFL from NASH.<sup>20,21</sup> This method is controversial because some studies illustrated that there is no significant difference in ALT and AST levels between patients with NAFL and NASH.<sup>22</sup> We found elevated ALT and AST levels in NAFL mice, but we could not use these two markers to distinguish NAFL and NASH. This preclinical evidence supports the idea that NAFL cannot be distinguished from NASH using ALT and AST alone.

LPS is a component of the cell wall of gram-negative bacteria. Alterations in intestinal flora caused by long-term consumption of a high-fat diet can lead to increased intestinal LPS levels. The absorption of intestinal LPS into peripheral blood can cause a slight increase in serum LPS levels called metabolic endotoxemia, which

is usually 10 to 50-fold lower than the level of endotoxemia found in septic shock.<sup>23–25</sup> When combined with CD14, LPS can activate the NF- $\kappa$ B signaling pathway and increase the levels of inflammatory factors that conspire to facilitate the development of fatty liver, obesity, and insulin resistance.<sup>26,27</sup> We found that NAFL mice have higher levels of LPS than normal mice and that NASH mice have higher levels than NAFL mice. This suggests that LPS levels increase with the progression of the severity of fatty liver disease, and serum LPS levels may be useful in distinguishing NASH from NAFL.

Intestinal flora diversity is an important aspect of maintaining intestinal flora homeostasis, which can regulate important health outcomes.<sup>28,29</sup> In this study, we used high-throughput 16S rRNA sequencing to analyze the fecal flora of our NAFLD mouse model. By examining  $\alpha$  and  $\beta$  diversity, we illustrated that the abundance and diversity of fecal flora in NAFL/NASH mice were lower than those in normal mice, and the flora composition also differed between NAFL/NASH and normal mice. However,  $\alpha$  and  $\beta$  diversity were similar between the NAFL and NASH groups. Further taxonomic analysis of fecal flora composition illustrated at the phylum level, Bacteroidetes, Firmicutes, Proteobacteria, Actinobacteria, and Saccharibacteria were most the common phyla in all groups of mice. However, we found an increased relative abundance of these groups in NAFL/NASH mice compared with that in normal mice. The relative abundance of other phyla (i.e., Bacteroidetes/Firmicutes) was lower in NAFL/NASH mice than in normal mice. These findings are consistent with prior reports.<sup>30–32</sup> It is believed that a lower abundance of Bacteroidetes might facilitate the metabolic dominance of other bacteria that are more efficient in extracting energy from the diet.<sup>33</sup> Our study also found that

the relative abundance of Actinobacteria, Saccharibacteria, and Proteobacteria also changed in NAFL/NASH mice. However, there were no obvious differences in the abundance of phyla that could distinguish the NAFL and NASH groups.

At the genus level, we found that the relative abundance of *Alloprevotella*, *Ruminococcaceae* UCG-014, *Ruminococcus* 1, and *Candidatus Saccharimonas* was lower in NAFL/NASH mice, whereas that of *Bifidobacterium*, *Faecalibaculum*, *Helicobacter*, *Eubacterium coprostanoligenes* group, and *Romboutsia* was increased. *Alloprevotella* and *Ruminococcaceae* UCG-014 are relatively common beneficial bacteria found in human and animal intestines that can promote the generation of short-chain fatty acids (SCFAs).<sup>34,35</sup> SCFAs can regulate energy extraction from the diet, help maintain energy homeostasis, nourish intestinal epithelial cells, and decrease the levels of blood LPS or other inflammatory factors, thereby decreasing intestinal permeability.<sup>36</sup> *Ruminococcus* 1 is a highly heterogeneous genus in which some species have probiotic effects,<sup>36</sup> whereas others are considered pathogenic. A prior study found a positive correlation between the abundance of *Romboutsia* and obesity,<sup>37</sup> suggesting that these bacteria play a negative role in lipid metabolism. Interestingly, *Faecalibaculum*, a genus believed to promote the beneficial generation of SCFAs in the intestines,<sup>38</sup> had an increased relative abundance in NAFL/NASH mice, as did *Bifidobacterium*, a genus that has long been considered a probiotic. *Bifidobacterium* can competitively occupy the surface of the intestinal mucosa, preventing the invasion of pathogenic bacteria and reducing the absorption of LPS.<sup>39-41</sup> Thus, the unexpectedly high abundance of *Faecalibaculum* and *Bifidobacterium* in NAFL/NASH mice merit further investigation.

We also identified changes in the relative abundance of four genera that helped differentiate NAFL and NASH mice. *Lactobacillus* was relatively less abundant in the NASH group than in the NAFL group, whereas *Desulfovibrio*, *Ruminiclostridium* 9, and *Turicibacter* were more abundant. The AUROCs of all four genera exceeded 0.7, with the highest AUROC belonging to *Turicibacter* (AUROC = 0.937). These data suggest that the relative abundance of these four genera has potential value for NASH diagnosis, particularly when trying to distinguish it from NAFL. We also performed Spearman's correlation analysis, which illustrated that NAS was positively correlated with the relative abundance of *Desulfovibrio*, *Ruminiclostridium* 9, and *Turicibacter*. This indicates that the relative abundance of these three genera could be used as surrogates for assessing NAFLD severity and thereby further helping to distinguish NASH from NAFL. *Lactobacillus* is often used as a probiotic in the clinic, and this genus includes more than 180 species, many of which can generate SCFAs. *Lactobacillus* can also improve epithelial barrier function and regulate immune response,<sup>42</sup> making it unsurprising that its abundance decreased with disease progression. *Desulfovibrio* comprises a group of gram-negative endotoxin-producing bacteria, and an increased abundance of *Desulfovibrio* in the intestine has been associated with increased levels of inflammatory blood markers.<sup>38</sup> This role is also consistent with our data and the relative abundance of this genus in NASH. Although *Turicibacter*, the genus most strongly correlated with NASH, is commonly detected in the intestines and feces of humans and animals, its role in the intestinal microecology and its pathogenic potential remain unclear.<sup>43</sup>

This study had several limitations. First, the structural characteristics of the mouse intestinal flora in NAFL/NASH may be different from that of humans. Additionally, although some variations in fecal flora were found in mice with NAFL/NASH, the pathogenic mechanisms of these bacteria in NAFLD are still unknown. Third, the changed bacteria are also associated with obesity, hyperlipidemia, insulin resistance, and metabolic syndrome. Further research is needed to identify the specific factors and mechanism.

In summary, we established a mouse model of NAFLD using a high-fat/high-sugar diet. NAFLD mice displayed changes in blood lipid levels, FBG levels, liver function, LPS levels, and the fecal flora structure, consistent with some aspects of human disease. Moreover, we identified increased serum LPS levels and differences in the relative abundance of *Lactobacillus*, *Desulfovibrio*, *Ruminiclostridium 9*, and *Turicibacter* as features that may help differentiate NASH from NAFL. Moreover, the relative abundance of *Desulfovibrio*, *Ruminiclostridium 9*, and *Turicibacter* was positively correlated with NAS, suggesting that evaluation of these species may be helpful in understanding the severity of NAFLD. Together, these data may provide non-invasive biomarkers for distinguishing NASH from NAFL and clinically assessing NAFLD.

#### Declaration of conflicting interest

The authors declare that there is no conflict of interest.

#### Funding

This work was supported by the Logistics Scientific Research Project of PLA (No. CHJ12J027 to Lihong Cui), National Natural Science Foundation of China (No. 82070553 to Lihong Cui), and Capital Health Research and

Development of Special Fund Program (No. 2020-2-5113 to Lihong Cui).

#### ORCID iD

Lihong Cui  <https://orcid.org/0000-0003-3007-728X>

#### References

1. Yilmaz Y and Younossi ZM. Obesity-associated nonalcoholic fatty liver disease. *Clin Liver Dis* 2014; 18: 19–31. doi: 10.1016/j.cld.2013.09.018.
2. Higuera-De La Tijera F and Servin-Caamano AI. Pathophysiological mechanisms involved in non-alcoholic steatohepatitis and novel potential therapeutic targets. *World J Hepatol* 2015; 7: 1297–1301. doi: 10.4254/wjh.v7.i10.1297.
3. De Luca-Johnson J, Wangenstein KJ, Hanson J, et al. Natural History of Patients Presenting with Autoimmune Hepatitis and Coincident Nonalcoholic Fatty Liver Disease. *Dig Dis Sci* 2016; 61: 2710–2720. doi: 10.1007/s10620-016-4213-3.
4. Fan JG and Farrell GC. Epidemiology of non-alcoholic fatty liver disease in China. *J Hepatol* 2009; 50: 204–210. doi: 10.1016/j.jhep.2008.10.010.
5. Caldwell S and Argo C. The natural history of non-alcoholic fatty liver disease. *Dig Dis* 2010; 28: 162–168. doi: 10.1159/000282081.
6. Cohen JC, Horton JD and Hobbs HH. Human fatty liver disease: old questions and new insights. *Science* 2011; 332: 1519–1523. doi: 10.1126/science.1204265.
7. Yang JY and Kweon MN. The gut microbiota: a key regulator of metabolic diseases. *BMB Rep* 2016; 49: 536–541. doi: 10.5483/bmbrep.2016.49.10.144.
8. Fialho A, Fialho A, Thota P, et al. Small Intestinal Bacterial Overgrowth Is Associated with Non-Alcoholic Fatty Liver Disease. *J Gastrointest Liver Dis* 2016; 25: 159–165. doi: 10.15403/jgld.2014.1121.252.iwg.
9. Sohn W, Jun DW, Lee KN, et al. *Lactobacillus paracasei* Induces M2-Dominant Kupffer Cell Polarization in a Mouse Model of Nonalcoholic

- Steatohepatitis. *Dig Dis Sci* 2015; 60: 3340–3350. doi: 10.1007/s10620-015-3770-1.
10. Cani PD and Delzenne NM. The gut microbiome as therapeutic target. *Pharmacol Ther* 2011; 130: 202–212. doi: 10.1016/j.pharmthera.2011.01.012.
  11. Gangarapu V, Ince AT, Baysal B, et al. Efficacy of rifaximin on circulating endotoxins and cytokines in patients with nonalcoholic fatty liver disease. *Eur J Gastroenterol Hepatol* 2015; 27: 840–845. doi: 10.1097/MEG.0000000000000348.
  12. Brunt EM. Pathology of nonalcoholic fatty liver disease. *Nat Rev Gastroenterol Hepatol* 2010; 7: 195–203. doi: 10.1038/nrgastro.2010.21.
  13. Matteoni CA, Younossi ZM, Gramlich T, et al. Nonalcoholic fatty liver disease: a spectrum of clinical and pathological severity. *Gastroenterology* 1999; 116: 1413–1419. doi: 10.1016/s0016-5085(99)70506-8.
  14. Kleiner DE, Brunt EM, Van Natta M, et al. Design and validation of a histological scoring system for nonalcoholic fatty liver disease. *Hepatology* 2005; 41: 1313–1321. doi: 10.1002/hep.20701.
  15. Cole JR, Wang Q, Cardenas E, et al. The Ribosomal Database Project: improved alignments and new tools for rRNA analysis. *Nucleic Acids Res* 2009; 37: D141–D145. doi: 10.1093/nar/gkn879.
  16. Wang Y, Sheng HF, He Y, et al. Comparison of the levels of bacterial diversity in freshwater, intertidal wetland, and marine sediments by using millions of illumina tags. *Appl Environ Microbiol* 2012; 78: 8264–8271. doi: 10.1128/AEM.01821-12.
  17. Jiang XT, Peng X, Deng GH, et al. Illumina sequencing of 16S rRNA tag revealed spatial variations of bacterial communities in a mangrove wetland. *Microb Ecol* 2013; 66: 96–104. doi: 10.1007/s00248-013-0238-8.
  18. Araujo AR, Rosso N, Bedogni G, et al. Global epidemiology of non-alcoholic fatty liver disease/non-alcoholic steatohepatitis: What we need in the future. *Liver Int* 2018; 38: 47–51. doi: 10.1111/liv.13643.
  19. Trauner M, Arrese M and Wagner M. Fatty liver and lipotoxicity. *Biochim Biophys Acta* 2010; 1801: 299–310. doi: 10.1016/j.bbali.2009.10.007.
  20. Chalasani N, Younossi Z, Lavine JE, et al. The diagnosis and management of nonalcoholic fatty liver disease: Practice guidance from the American Association for the Study of Liver Diseases. *Hepatology* 2018; 67: 328–357. doi: 10.1002/hep.29367.
  21. Review T, LaBrecque DR, Abbas Z, et al. World Gastroenterology Organisation global guidelines: Nonalcoholic fatty liver disease and nonalcoholic steatohepatitis. *J Clin Gastroenterol* 2014; 48: 467–473. doi: 10.1097/MCG.0000000000000116.
  22. Ma X, Liu S, Zhang J, et al. Proportion of NAFLD patients with normal ALT value in overall NAFLD patients: a systematic review and meta-analysis. *BMC Gastroenterol* 2020; 20: 10. doi: 10.1186/s12876-020-1165-z.
  23. Yokota A, Fukuya S, Islam KB, et al. Is bile acid a determinant of the gut microbiota on a high-fat diet? *Gut Microbes* 2012; 3: 455–459. doi: 10.4161/gmic.21216.
  24. Chakraborti CK. New-found link between microbiota and obesity. *World J Gastrointest Pathophysiol* 2015; 6: 110–119. doi: 10.4291/wjgp.v6.i4.110.
  25. Mehrpouya-Bahrami P, Chitralla KN, Ganewatta MS, et al. Blockade of CB1 cannabinoid receptor alters gut microbiota and attenuates inflammation and diet-induced obesity. *Sci Rep* 2017; 7: 15645. doi: 10.1038/s41598-017-15154-6.
  26. Saad MJ, Santos A and Prada PO. Linking Gut Microbiota and Inflammation to Obesity and Insulin Resistance. *Physiology (Bethesda)* 2016; 31: 283–293. doi: 10.1152/physiol.00041.2015.
  27. Liu J, Batkai S, Pacher P, et al. Lipopolysaccharide induces anandamide synthesis in macrophages via CD14/MAPK/phosphoinositide 3-kinase/NF-kappaB independently of platelet-activating factor. *J Biol Chem* 2003; 278: 45034–45039. doi: 10.1074/jbc.M306062200.
  28. Gill SR, Pop M, Deboy RT, et al. Metagenomic analysis of the human distal gut microbiome. *Science* 2006; 312: 1355–1359. doi: 10.1126/science.1124234.
  29. Lozupone CA, Stombaugh JI, Gordon JI, et al. Diversity, stability and resilience of

- the human gut microbiota. *Nature* 2012; 489: 220–230. doi: 10.1038/nature11550.
30. Raman M, Ahmed I, Gillevet PM, et al. Fecal microbiome and volatile organic compound metabolome in obese humans with nonalcoholic fatty liver disease. *Clin Gastroenterol Hepatol* 2013; 11: 868–875.e1-3. doi: 10.1016/j.cgh.2013.02.015.
  31. Turnbaugh PJ, Ley RE, Mahowald MA, et al. An obesity-associated gut microbiome with increased capacity for energy harvest. *Nature* 2006; 444: 1027–1031. doi: 10.1038/nature05414.
  32. Ley RE, Backhed F, Turnbaugh P, et al. Obesity alters gut microbial ecology. *Proc Natl Acad Sci USA* 2005; 102: 11070–11075. doi: 10.1073/pnas.0504978102.
  33. Mouzaki M, Comelli EM, Arendt BM, et al. Intestinal microbiota in patients with non-alcoholic fatty liver disease. *Hepatology* 2013; 58: 120–127. doi: 10.1002/hep.26319.
  34. Song JJ, Tian WJ, Kwok LY, et al. Effects of microencapsulated *Lactobacillus plantarum* LIP-1 on the gut microbiota of hyperlipidaemic rats. *Br J Nutr* 2017; 118: 481–492. doi: 10.1017/S0007114517002380.
  35. Scott KP, Martin JC, Duncan SH, et al. Prebiotic stimulation of human colonic butyrate-producing bacteria and bifidobacteria, in vitro. *FEMS Microbiol Ecol* 2014; 87: 30–40. doi: 10.1111/1574-6941.12186.
  36. Cani PD, Possemiers S, Van De Wiele T, et al. Changes in gut microbiota control inflammation in obese mice through a mechanism involving GLP-2-driven improvement of gut permeability. *Gut* 2009; 58: 1091–1103. doi: 10.1136/gut.2008.165886.
  37. Hu S, Xu Y, Gao X, et al. Long-Chain Bases from Sea Cucumber Alleviate Obesity by Modulating Gut Microbiota. *Mar Drugs* 2019; 17: 455. doi: 10.3390/md17080455.
  38. Gibson GR. Physiology and ecology of the sulphate-reducing bacteria. *J Appl Bacteriol* 1990; 69: 769–797. doi: 10.1111/j.1365-2672.1990.tb01575.x.
  39. Serafini F, Strati F, Ruas-Madiedo P, et al. Evaluation of adhesion properties and anti-bacterial activities of the infant gut commensal *Bifidobacterium bifidum* PRL2010. *Anaerobe* 2013; 21: 9–17. doi: 10.1016/j.anaerobe.2013.03.003.
  40. Xiang L, Peng LL, Du WX, et al. Protective effects of *Bifidobacterium* on intestinal barrier function in LPS-induced enterocyte barrier injury of Caco-2 monolayers and in a rat NEC model. *Plos One* 2016; 11(8): e0161635. doi:10.1371/journal.pone.0161635.
  41. Pokusaeva K, Fitzgerald GF and van Sinderen D. Carbohydrate metabolism in *Bifidobacteria*. *Genes Nutr* 2011; 6: 285–306. doi: 10.1007/s12263-010-0206-6.
  42. Lebeer S, Vanderleyden J and De Keersmaecker SC. Genes and molecules of lactobacilli supporting probiotic action. *Microbiol Mol Biol Rev* 2008; 72: 728–764, Table of Contents. doi: 10.1128/MMBR.00017-08.
  43. Auchtung TA, Holder ME, Gesell JR, et al. Complete Genome Sequence of *Turicibacter* sp. Strain H121, Isolated from the Feces of a Contaminated Germ-Free Mouse. *Genome Announc* 2016; 4: e00114–16. doi: 10.1128/genomeA.00114-16.